Biophysical *Journal*
Biophysical Letter

Biophysical Society

Tension and Elasticity Contribute to Fibroblast Cell Shape in Three Dimensions

Christoph A. Brand,[1,2] Marco Linke,[1,2] Kai Weißenbruch,[3,4] Benjamin Richter,[3] Martin Bastmeyer,[3,4,5,*] and Ulrich S. Schwarz[1,2,5,*]

[1]BioQuant-Center for Quantitative Biology and [2]Institute for Theoretical Physics, Heidelberg University, Heidelberg, Germany; [3]Cell and Neurobiology, Zoological Institute and [4]Institute of Functional Interfaces (IFG), Karlsruhe Institute of Technology (KIT), Karlsruhe, Germany; and [5]HEiKA – Heidelberg Karlsruhe Research Partnership, Heidelberg University, Karlsruhe Institute of Technology (KIT), Karlsruhe, Germany

ABSTRACT The shape of animal cells is an important regulator for many essential processes such as cell migration or division. It is strongly determined by the organization of the actin cytoskeleton, which is also the main regulator of cell forces. Quantitative analysis of cell shape helps to reveal the physical processes underlying cell shape and forces, but it is notoriously difficult to conduct it in three dimensions. Here we use direct laser writing to create 3D open scaffolds for adhesion of connective tissue cells through well-defined adhesion platforms. Due to actomyosin contractility in the cell contour, characteristic invaginations lined by actin bundles form between adjacent adhesion sites. Using quantitative image processing and mathematical modeling, we demonstrate that the resulting shapes are determined not only by contractility, but also by elastic stress in the peripheral actin bundles. In this way, cells can generate higher forces than through contractility alone.

The behavior of eukaryotic cells is strongly determined by extracellular signals, including the adhesive, geometrical, topographical, and mechanical properties of the extracellular matrix (1). Micropatterning of cell environments has emerged as a powerful method to normalize and quantitatively investigate the shape, organization, forces, and behavior of adherent cells as a function of external guidance cues (2). However, it remains a challenge to extend these approaches into three dimensions (3). A 3D environment is physiologically more relevant and provides different guidance cues than a 2D environment. It might also lead to different mechanisms of force generation than in 2D.

Here we address the question which physical factors determine cell shape and forces in connective tissue-like 3D environments, when cells typically attach at a few adhesion sites anchored in an open scaffold (4). During recent years, direct laser writing has emerged as a powerful technique to create controlled environments for 3D cell culture (5,6). Using a femtosecond pulsed laser for two-photon polymerization in a protein-repellent photoresist, we created 3D microscaffolds that consist of five pillars (diameter 5 μm) of identical height (25 μm), which were separated by a distance of 10 μm and arranged around a central pillar of lesser height (15 μm) (Fig. 1 *A*). We then created spatially well-defined and separated adhesion platforms of cubic shape using a second photoresist that could be functionalized with fibronectin (Fig. 1 *B*). Together these adhesive cubes form the shape of an inverted pyramid. NIH 3T3 fibroblasts were cultured in the scaffolds and adopted the shape of an inverted pyramid in these structures, with strong invaginations between the adhesive cubes. Fig. 1 *C* shows a scanning electron micrograph of a cell in a scaffold in which one pillar has been moved out to achieve variation in cell shape. For this study, we used offsets of 1.5, 2.5, 4.5, 5, and 7.5 μm. Fig. 1 *D* shows a 3D volume rendering of a cell in the regular scaffold without crossbars using the image data for actin (*green*), fibronectin (*red*), and chromatin (*blue*) as well as for the micropillars (*gray*). Additional fluorescence images of two other cells, one viewed from above showing all channels (Fig. 1 *E*) and one from below using only the actin channel (Fig. 1 *F*), illustrate that the cells adopt a pyramidal shape and span between all available adhesive cubes. Experiments with different designs showed that this geometry is favorable for stable cell adhesion.

The most striking feature of the images presented in Fig. 1 would be the invaginated arcs that form between

Submitted April 11, 2017, and accepted for publication June 30, 2017.

*Correspondence: martin.bastmeyer@kit.edu or ulrich.schwarz@bioquant.uni-heidelberg.de

Christoph A. Brand, Marco Linke, and Kai Weißenbruch contributed equally to this work.

Editor: Jason Swedlow.

http://dx.doi.org/10.1016/j.bpj.2017.06.058

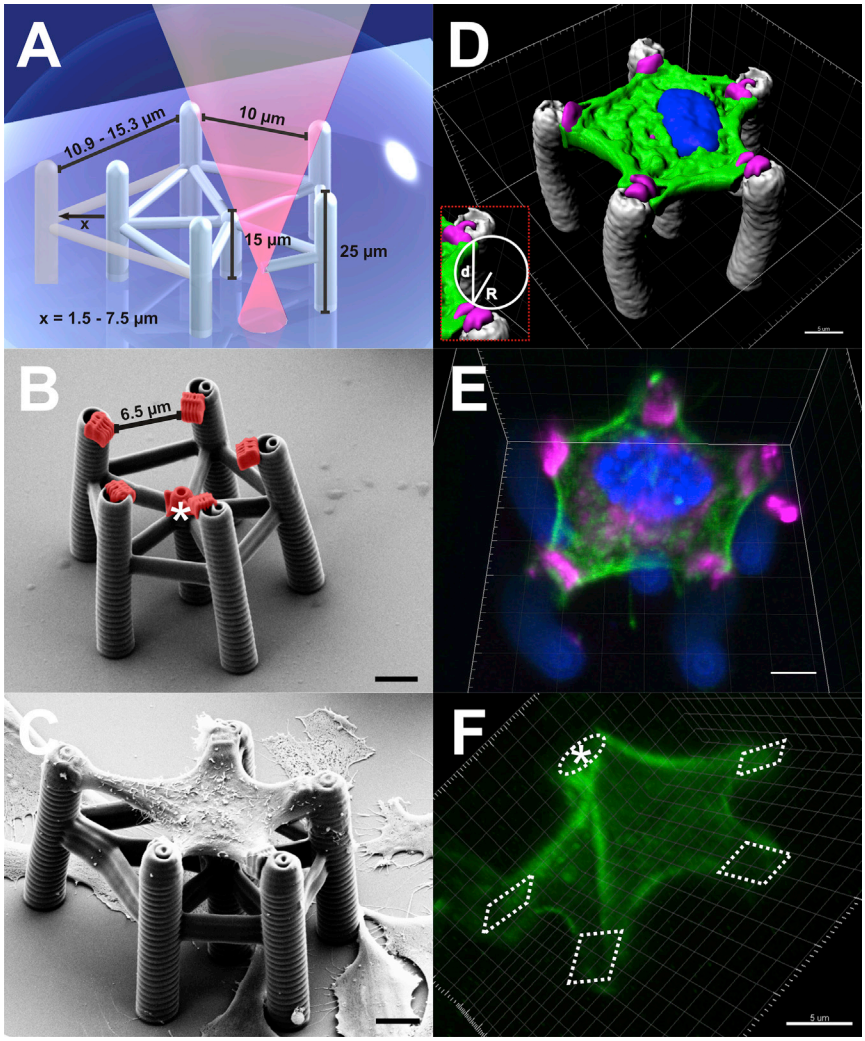

FIGURE 1 Experimental setup and cell shape. (*A*) 3D microscaffolds for cell culture were created with direct laser writing. (*B* and *C*) Given here are scanning electron micrographs. (*B*) The six adhesive cubes (pseudocolored in *red*) form an inverted pyramid with a fivefold basis. The shortest distance between two neighboring adhesions and the central adhesion are both marked. (*C*) Given here is an image of a cell adhering to a 3D scaffold. One pillar is moved out to achieve variation in cell shape. (*D–F*) Volume rendering and fluorescence images illustrate that all adhesion points are used. (*D*) Rendering shows actin (*green*), chromatin (*blue*), fibronectin (*violet*), and micropillars (*gray*). (*E*) Fluorescence image includes labels for actin (*green*), fibronectin (*violet*), and chromatin (*blue*). (*F*) Fluorescence image (actin channel) of a cell viewed from below is given, showing that the cell obtains the shape of an inverted pyramid. Scale bars represent 5 μm. To see this figure in color, go online.

neighboring adhesive cubes and that are best visible in Fig. 1, *E* and *F*, as inward curved actin bundles running from one adhesive cube to the next. These bundles are similar to the peripheral stress fibers often visible in 2D cell culture (7–9). They appear with high regularity in the *x-y* plane, where they are tilted out of the horizontal plane because the lower adhesion point pulls the whole cell downwards. For the arcs that span between the outer adhesion sites and the lower central pillar, the *z* resolution makes it often difficult to segment them in detail. Visual inspection shows that sometimes they are missing (like one in Fig. 1 *F*) and that they are often weaker in actin intensity.

For cell adhesion on 2D homogeneous substrates, it has been observed in the past that cells often form invaginated arcs that are surprisingly circular (7,8). Culturing mouse melanoma (B16–F1) cells and buffalo rat liver cells on 2D adhesive dot patterns revealed that the arc radius increases roughly linear with the spanning distance between the dots (9). This can be explained by the 2D tension-elasticity model (TEM) (9–12). The 2D TEM is a contour model that considers cell shape projected onto the *x-y* plane. It starts from the assumption that myosin II-based contractility leads to tensions in the cortex (surface tension σ) and in the actin arcs (line tension λ) that both do not depend on absolute distances, because the myosin II motors locally slide along the actin filaments. Balancing the two types of tension thus can explain circular arcs with radius $R = \lambda/\sigma$, but not the dependence on the spanning distance d. Because elastic effects depend on absolute distances, the distance dependence can be explained by assuming an elastic line tension $\lambda = EA(L - L_0)/L_0$, with EA being the 1D elastic modulus, L the contour length, and L_0 the resting length. For simplicity, in the following we assume $L_0 = d$, that is, the straight fiber is assumed to be the relaxed case. Using the geometrical relation among L, d, and R, we obtain the equations of the 2D TEM,

$$R = l_f\left(\frac{2R}{d}\arcsin\left(\frac{d}{2R}\right) - 1\right) \approx 24^{-1/3} l_f^{1/3} d^{2/3}, \quad (1)$$

where $l_f = EA/\sigma$ is a length scale defined by the interplay between 1D elastic modulus EA and 2D surface tension σ. Whereas the first equation is self-consistent and can be solved only numerically, the second equation follows in the limit of a flat arc, $d \ll R$. Both equations give an increasing arc radius R as a function of spanning distance d.

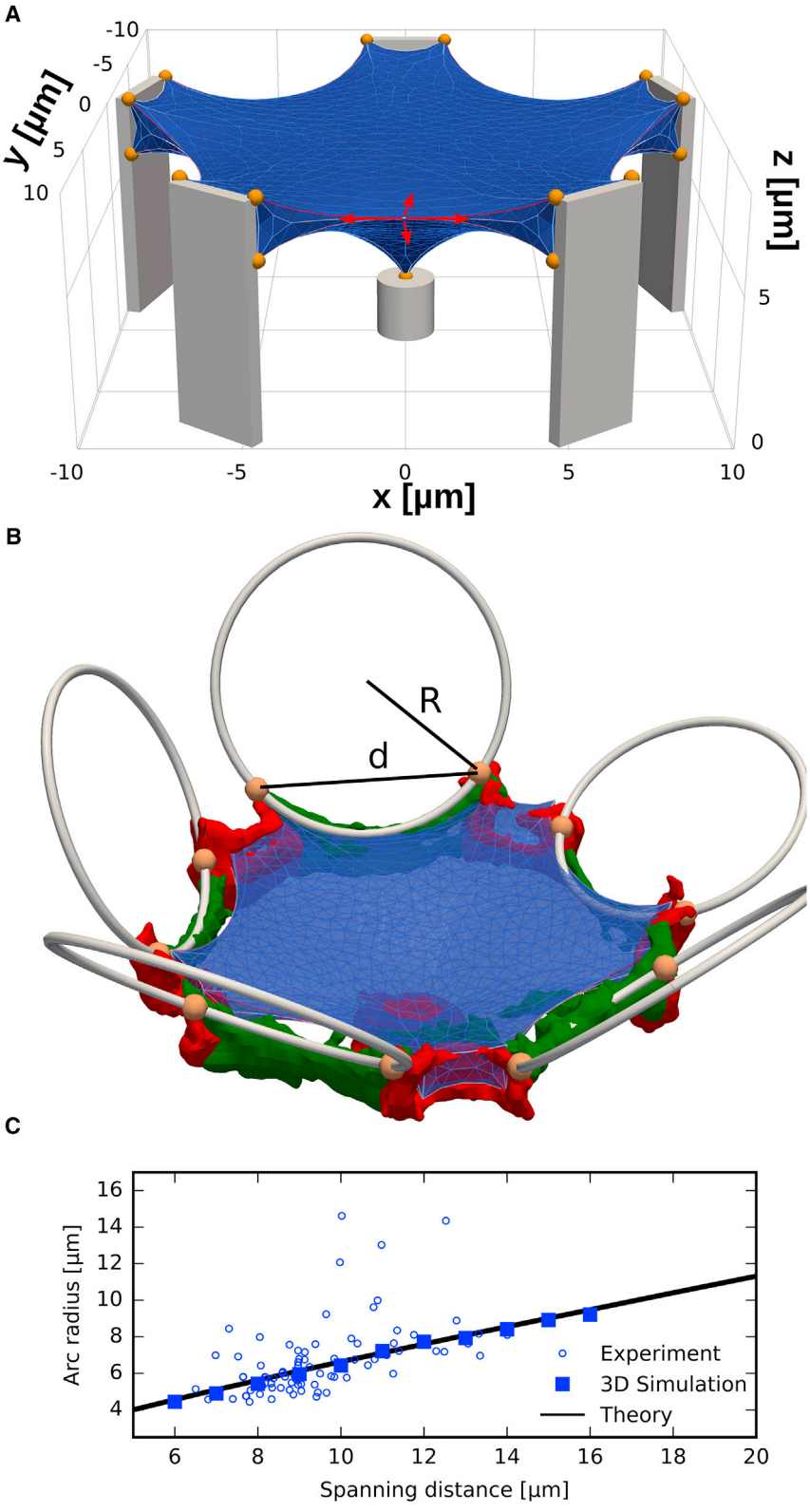

FIGURE 2 Quantitative analysis and modeling. (*A*) Given here is a computational 3D model of a contracted cell in the scaffold from Fig. 1 (*gray*) with adhesion sites marked (*yellow spheres*). The vector arrows show the force balance at the convoluted cell envelope in 3D. (*B*) Given here is an overlay with the segmented cell structure and the tilted circles fitted to the actin arcs. Segmented F-actin (*green*), fibronectin (*red*), and anchoring points of fitted circles (*yellow spheres*) are shown. (*C*) Both the computer simulations and the 2D tension-elasticity model (TEM) describe the experimentally measured increasing relation between spanning distance *d* and arc radius *R*. To see this figure in color, go online.

We first verified that the 2D TEM from Eq. 1 also applies for 3T3 fibroblasts in 2D (Fig. S1). Quantitative image processing (for details, see the Supporting Material) revealed that arc radius R indeed increases roughly linear with spanning distance d (Fig. S2), as reported before for B16-F1 and buffalo rat liver cells on micropatterns. Fitting the full 2D TEM to the experimental 2D data gave $l_f = 263 \pm 35$ μm. For a typical surface tension $\sigma = 2$ nN/μm (10), this corresponds to an elastic 1D modulus of $EA = l_f\sigma = 526$ nN. The good agreement between the 2D experimental data and the 2D TEM suggests that in 2D, cells use not only myosin II-based contractility, but also elastic stress to generate forces. This elastic stress could be sustained not only by myosin II itself, which also acts as an actin cross-linker, but also by, e.g., α-actinin, which is a very prominent component of mature stress fibers (13).

Whereas in 2D the ventral and dorsal parts of the actin cortex pull in the same direction and together generate the effective surface tension σ, in 3D the cortex around an invaginated arc has a more convoluted shape. We therefore created a full 3D computational model for cell shape extending our earlier work for actively contracting 2D cable networks to 3D (9,11). In our 3D model, the surface energy of a triangulated network of active cables is minimized numerically (for details, see the Supporting Material). Like the 2D TEM, it also combines tension and elasticity, but it does not make any assumption on where the actin bundles will appear, because in contrast to 2D, there is no contracting boundary that can be identified clearly from the outset. Fig. 2 *A* shows the results of the computer simulation for the adhesion geometry used in Fig. 1. Interestingly, in the model the elastic stress is found to be sharply located to the lines directly connecting neighboring sites of adhesion (Fig. S4). This is exactly the location where the strong peripheral actin bundles are found in the experiments. This striking agreement suggests a mechanosensitive response of the actin cytoskeleton to mechanical stress in the cortex that develops in response to the external adhesive cues. Further, the model predicts that the mechanical force between two adhesion cubes in the x-y plane is considerably higher (>5 nN) than the mechanical force on the connection of an outer adhesion cube to the central one (<2 nN). Because we experimentally observe these arcs to be weaker (Fig. S5), this prediction supports our conclusion that SFs are more likely to form where the cell is to bear high forces.

Fig. 2 *A* shows that in general, we obtain good agreement between the simulated and the measured fibroblast cell shapes. For a quantitative analysis, we next fitted tilted circles to the fluorescent data, as shown in Fig. 2 *B* (for details, see the Supporting Material). Fig. 2 *C* shows that experimentally, we find that arc radius R increases with spanning distance d also in 3D (*dot symbols*, $N_{\text{cells}} = 35, N_{\text{arcs}} = 81$). The anchor points (*yellow spheres* in Fig. 2 *B*) of the arcs are not always located exactly at the shortest distance between two adhesive cubes (compare Fig. 1 *B*), which causes the quasi-continuous distribution of spanning distances. In general, both in 2D and 3D we find large variability due to the individual spreading history of every cell.

We next simulated the R-d relation in our 3D computational model for parameters that correspond to $l_f = 50$ μm. As shown in Fig. 2 *C*, we find a roughly linear relation in good agreement with the experimental data. A fit of the experimental data to the 2D TEM from Eq. 1 gives $l_f = 35 \pm 2.6$ μm (Fig. 2 *C*). The small effective values of $l_f = EA/\sigma$ indicates that fibroblast cells in 3D are either more contractile (larger σ) or that the actin arcs in 3D are weaker (smaller EA), or both. We speculate that the effect of weaker arcs dominates, because the computational model shows that the two parts of the actin cortex pulling at the peripheral actin fibers partially compensate each other in a nonplanar geometry (Fig. 2 *A*), which should lead to weaker mechanosensitive growth of the actin fibers. In fact, a similar effect of smaller arc radii R has been observed before in 2D when inhibiting myosin II contractility with blebbistatin (9). With the value for the surface tension σ from above, we now would have an elastic 1D modulus of only $EA = l_f\sigma = 70$ nN.

In the future, live cell imaging, pharmacological treatments, controlled release of adhesion platforms, and deformable scaffolds might be used to investigate the mechanisms of arc formation and force generation in open 3D scaffolds in more detail. The data presented here establish that cell forces in 3D environments are based not only on myosin II-based contractility, but also on cross-linker-based elasticity. These results agree with recent reports of strongly elastic effects in cellular force generation (14,15) and suggest that also in 3D, cells use elastic prestress to generate higher forces than based on contractility alone.

SUPPORTING MATERIAL

Supporting Materials and Methods and five figures are available at http://www.biophysj.org/biophysj/supplemental/S0006-3495(17)30742-7.

AUTHOR CONTRIBUTIONS

M.B. and U.S.S. designed the research and supervised the project. C.A.B. and M.L. performed the computer simulations and the image processing. K.W. and B.R. performed the experiments. C.A.B., M.L., and U.S.S. wrote the manuscript with help from K.W. and M.B.

ACKNOWLEDGMENTS

M.B. and B.R. acknowledge support from the German Research Council (BA-1034/16-1). U.S.S. is a member of the Interdisciplinary Center for Scientific Computing (IWR) and of the Cluster of Excellence CellNetworks at Heidelberg.

REFERENCES

1. Geiger, B., J. P. Spatz, and A. D. Bershadsky. 2009. Environmental sensing through focal adhesions. *Nat. Rev. Mol. Cell Biol.* 10:21–33.
2. Ruprecht, V., P. Monzo, …, V. Viasnoff. 2017. How cells respond to environmental cues—insights from bio-functionalized substrates. *J. Cell Sci.* 130:51–61.
3. Baker, B. M., and C. S. Chen. 2012. Deconstructing the third dimension: how 3D culture microenvironments alter cellular cues. *J. Cell Sci.* 125:3015–3024.
4. Griffith, L. G., and M. A. Swartz. 2006. Capturing complex 3D tissue physiology in vitro. *Nat. Rev. Mol. Cell Biol.* 7:211–224.
5. Klein, F., B. Richter, …, M. Bastmeyer. 2011. Two-component polymer scaffolds for controlled three-dimensional cell culture. *Adv. Mater.* 23:1341–1345.
6. Greiner, A. M., F. Klein, …, M. Bastmeyer. 2015. Cell type-specific adaptation of cellular and nuclear volume in micro-engineered 3D environments. *Biomaterials.* 69:121–132.
7. Zand, M. S., and G. Albrecht-Buehler. 1989. What structures, besides adhesions, prevent spread cells from rounding up? *Cell Motil. Cytoskeleton.* 13:195–211.
8. Bar-Ziv, R., T. Tlusty, …, A. Bershadsky. 1999. Pearling in cells: a clue to understanding cell shape. *Proc. Natl. Acad. Sci. USA.* 96:10140–10145.
9. Bischofs, I. B., F. Klein, …, U. S. Schwarz. 2008. Filamentous network mechanics and active contractility determine cell and tissue shape. *Biophys. J.* 95:3488–3496.
10. Bischofs, I. B., S. S. Schmidt, and U. S. Schwarz. 2009. Effect of adhesion geometry and rigidity on cellular force distributions. *Phys. Rev. Lett.* 103:048101.
11. Guthardt Torres, P., I. B. Bischofs, and U. S. Schwarz. 2012. Contractile network models for adherent cells. *Phys. Rev. E Stat. Nonlin. Soft Matter Phys.* 85:011913.
12. Labouesse, C., A. B. Verkhovsky, …, B. Vianay. 2015. Cell shape dynamics reveal balance of elasticity and contractility in peripheral arcs. *Biophys. J.* 108:2437–2447.
13. Hu, S., K. Dasbiswas, …, A. D. Bershadsky. 2017. Long-range self-organization of cytoskeletal myosin II filament stacks. *Nat. Cell Biol.* 19:133–141.
14. Sunyer, R., V. Conte, …, X. Trepat. 2016. Collective cell durotaxis emerges from long-range intercellular force transmission. *Science.* 353:1157–1161.
15. Oakes, P. W., E. Wagner, …, M. L. Gardel. 2017. Optogenetic control of RhoA reveals zyxin-mediated elasticity of stress fibres. *Nat. Commun.* 8:15817.